NASA Technical Memorandum 105371

Thermal and Solutal Convection With Conduction Effects Inside a Rectangular Enclosure

Christophe Mennetrier and Walter M.B. Duval
Lewis Research Center
Cleveland, Ohio

December 1991

NASA

THERMAL AND SOLUTAL CONVECTION WITH CONDUCTION EFFECTS INSIDE A RECTANGULAR ENCLOSURE

*Christophe Mennetrier * and Walter M. B. Duval*

NASA Lewis Research Center
Cleveland, Ohio 44135

ABSTRACT

We investigate numerically the effects of various boundary conditions on the flow field characteristics of the Physical Vapor Transport process. We use a prescribed temperature profile as boundary condition on the enclosure walls, and we consider parametric variations applicable to ground-based and space microgravity conditions. For ground-based applications, density gradients in the fluid phase generate buoyancy-driven convection which in turn disrupts the uniformity of the mass flux at the interface depending on the orientation. Heat conduction in the crystal can affect the fluid flow near the interface of the crystal. When considering isothermal source and sink at the interfaces, we observe a diffusive mode and three convective modes (i.e., thermal, solutal and thermo-solutal). The convective modes show opposing flow field trends between thermal and solutal convection; theoretically, these trends can be used to achieve a uniform mass flux near the crystal. However, under the physical conditions chosen, the mathematical condition necessary for uniform mass flux cannot be satisfied because of thermodynamic restrictions. When a longitudinal thermal gradient is prescribed on the boundary of the crystal a non-uniform interface temperature results, which induces a symmetrical fluid flow near the interface for the vertical case. For space microgravity applications, we show that the flow field is dominated by the Stefan wind and a uniform mass flux results at the interface.

* Visiting Research Associate, Ecole Nationale Superieure des Mines, France

NOMENCLATURE

a Constant term in the vapor pressure law (a=29.75)

Ar Aspect ratio, $\left[\frac{L}{H}\right]$

b Constant term in the vapor pressure law (b=11767.1K)

C_P Thermal heat capacity of the gas

D_{AB} Binary diffusion coefficient

f Functional relationship

F(x,y) Source and sink term, $\left[=\int \rho C_p u \frac{\partial T}{\partial y} dy\right]$

g Gravitational acceleration

g_0 Gravitational acceleration at sea level

Gr_t Thermal Grashof number, $\left[\frac{g\rho^2 H^3 \beta \Delta T}{\mu^2}\right]$

Gr_s Solutal Grashof number, $\left[\frac{g\rho^2 H^3 \alpha \Delta \omega_A}{\mu^2}\right]$

H Height of the enclosure

J_A Dimensionless mass flux of A $\left[J_A = \frac{\rho u(L+l,y)}{\rho u(L+l,y)_{max}}\right]$

J_{max} Dimensional mass flux of A $(mol/s-m^2)$ $(J_{max} = \rho u(L+l,y)_{max})$

J_T Total mass flux of A $\left[J_T = \int_0^H \rho(L+l,y)u(L+l,y)dy\right]$

k Thermal conductivity of the gas

K Degree Kelvin

L Vapor transport length

l Length of the crystal

---

* Visiting Research Associate, Ecole Nationale Superieure des Mines, France

M_i Molar mass of compound i

P Pressure

Pe Peclet number, $\left[\ln\left[\frac{P_B(L+l)}{P_B(l)}\right]\right]$

Pr Prandtl number, $\left[C_P\frac{\mu}{k}\right]$

R Perfect gas law constant ($R = 8.32\ kgm^2s^{-2}mol^{-1}K^{-1}$)

Sc Schmidt number, $\left[\frac{\mu}{\rho D_{AB}}\right]$

T Temperature

u Velocity in the x-direction

v Velocity in the y-direction

x^*, y^* Dimensionless coordinate axes $\left[\frac{x}{2L}, \frac{y}{2L}\right]$

Greek symbols

α Coefficient of solutal expansion

β Coefficient of thermal expansion

λ Thermal conductivity of the solid

μ Dynamic viscosity

ω_i Mass fraction of component i

ρ Density of the gas

θ Angle between the ampoule axis and the gravity vector

Subscripts

A Compound A

B Compound B

c Pertains to the crystal interface

s Pertains to the source interface

T Total

x Component in x direction

y Component in y direction

Superscripts

c Pertains to the crystal interface

s Pertains to the source interface

* Dimensionless

I. INTRODUCTION

A sealed ampoule containing source material is typically used to grow large single crystals of opto-electronic materials by the process of Physical Vapor Transport (PVT). In the mathematical formulation of the PVT process a two dimensional enclosure has been considered [1,4–9,11,14,18–20]. For our physical situation, we also consider a rectangular enclosure, but we include conduction effects in the crystal. In this case, represented in Figure 1, the nutrient is heated on one end, sublimes and transports toward the cooler end, where it condenses. This diffusive flow is known as advective flow or Stefan wind. However, since the process runs under an imposed thermal gradient, significant density gradients are possible; consequently, a naturally recirculating convective flow can occur in addition to this basic flow. These gradients can arise from both thermal gradients (causing thermal convection) and concentration gradients (inducing solutal convection).

In recent years, publications on crystal growth from the vapor phase have mainly focused on the study of thermal convection [1–4,8,10,19,20] and its effects on the nonplanar interfacial mass flux [8,11,19,20]. Most of the authors have included solutal convection in their formulation, with the use of the framework of the Boussinesq approximation; or, alternatively, prescribed their species boundary conditions. The study of the process with prescribed species boundary conditions allows the effect of thermal convection on the process to be studied independently [6–8,18–20]. Therefore, the predicted mass flux distributions at the interfaces are influenced almost entirely by thermal convection. Rosenberger et al. [4–9,11] investigated extensively combined thermo-solutal convection. But they were not concerned with the particular case of mercurous chloride for which solutal convection becomes dominant because of both high molecular mass and vapor pressure. Recently, Extremet et al. [18] have studied simultaneously the balanced effects of thermal and solutal convection in a multizone rectangular enclosure. In their analysis, they used the Boussinesq approximation and they showed that special kinds of behavior, such as multiple counter-rotating cells, result from the opposing flow field trends between solutal and thermal convection.

Heat transfer has a predominant role in convection occurring during crystal growth [19,20]. Previous studies have considered geometrically flat interfaces at a constant temperature. However, if there is a temperature gradient in the crystal, this could induce localized recirculating cells which would modify the mass flux along the interface. In addition, a curved crystal interface could itself play a role in inducing convection cells.

The main objective of this work is to study the effect of heat conduction in the crystal on the transport process during PVT for various imposed temperature profiles. We also investigate the opposing effects of thermal and solutal convection on the recirculation patterns, in an attempt to exploit these contrary trends to correct nonuniformities of mass flux at the growing interface in the case of combined thermo-solutal convection. In addition, we examine the mathematically necessary conditions which provide for the existence of unidirectional flow in light of thermodynamic considerations. The microgravity environment is considered as a means of suppressing recirculating flow in an effort to restore the process to diffusion-controlled conditions. Finally, we investigate the role of longitudinal thermal gradients on the boundary of the crystal, especially as it relates to mass flux distribution at the interface and convection patterns.

II. MATHEMATICAL MODEL

Following previous models, we consider a rectangular enclosure of height H, vapor transport length L, and crystal and source material length l, where l = L/2. This represents a two-dimensional cross-section of an infinitely wide PVT enclosure. The cavity's axis is inclined at an angle θ with respect to gravitational acceleration. The solid nutrient A exists at both sides of the ampoule in equal amounts. One side is at a temperature T_S (source), the other at a temperature T_C (sink, i.e., the growing interface). With $T_S > T_C$, the compound A sublimes from the source, is carried by a non-reacting buffer gas B, and condenses on the crystal interface. The source and sink interfaces are assumed to be geometrically flat. Their temperature is determined by a heat balance in the gas and the crystals. The temperatures of the source and the sink in contact with the enclosure walls and ends are either uniform in temperature or subjected to a linear thermal gradient. A linear temperature profile from T_S to T_C is assumed along the upper and lower walls. The thermal conditions at the interfaces impose thermodynamically the weight fraction of component A in equilibrium with the solid through the partial pressure of the gaseous phase of compound A:

$$P_A = e^{\left[a-\frac{b}{T}\right]} \tag{1}$$

We assume complete rejection of B on both interfaces, and bounding walls are impermeable to both components. The molecular weights of the two vapor components are different, specifically one being mercurous chloride (M_A = 472 g/mol), the other being argon (M_B = 40 g/mol). This will expand our study to include thermal as well as solutal convection. The viscosity, binary diffusion coefficient, and thermal conductivity are assumed to be concentration and temperature independent.

The transport in this enclosure is governed by the system of nonlinear, coupled conservation equations for mass (continuity), species and energy, and balance equation for momentum (Navier-Stokes). These equations are, respectively, in rectangular two-dimensional coordinates, and for steady-state conditions:

In the vapor, $(l < x < L+l\ ;\ 0 < y < H)$:

Continuity equation:

$$\frac{\partial(\rho u)}{\partial x} + \frac{\partial(\rho v)}{\partial y} = 0 \tag{2}$$

Navier-Stokes equation

Projection on the x axis:

$$\frac{\partial}{\partial x}(\rho uu) + \frac{\partial}{\partial y}(\rho vu) = -\frac{\partial P}{\partial x} + \mu\frac{\partial}{\partial x}\left[\frac{\partial u}{\partial x} - \frac{2}{3}\left[\frac{\partial u}{\partial x} + \frac{\partial v}{\partial y}\right]\right] + \mu\frac{\partial^2 v}{\partial y \partial x} + \mu\frac{\partial^2 u}{\partial y^2} + \rho g_x \tag{3}$$

Projection on the y axis:

$$\frac{\partial}{\partial x}(\rho u v) + \frac{\partial}{\partial y}(\rho vv) = -\frac{\partial P}{\partial y} + \mu\frac{\partial}{\partial y}\left[\frac{\partial v}{\partial y} - \frac{2}{3}\left[\frac{\partial u}{\partial x} + \frac{\partial v}{\partial y}\right]\right] + \mu\frac{\partial^2 u}{\partial x \partial y} + \mu\frac{\partial^2 v}{\partial x^2} + \rho g_y \tag{4}$$

Conservation of species equation:

$$\frac{\partial}{\partial x}(\rho u\,\omega_i) + \frac{\partial}{\partial y}(\rho v\omega_i) = \frac{\partial}{\partial x}\left[\rho D_{AB}\frac{\partial \omega_i}{\partial x}\right] + \frac{\partial}{\partial y}\left[\rho D_{AB}\frac{\partial \omega_i}{\partial y}\right] \tag{5}$$

Conservation of energy in the fluid phase:

$$\frac{\partial}{\partial x}(\rho u C_P T) + \frac{\partial}{\partial y}(\rho v C_P T) = \frac{\partial}{\partial x}\left[k\frac{\partial T}{\partial x}\right] + \frac{\partial}{\partial y}\left[k\frac{\partial T}{\partial y}\right] \tag{6}$$

and in the solid, $(0 < x < l\ ;\ L+l < x < L+2l\ ;\ 0 < y < H)$:

$$\frac{\partial^2 T}{\partial x^2} + \frac{\partial^2 T}{\partial y^2} = 0 \tag{7}$$

Boundary conditions:

On the upper and lower walls, ($l < x < L+l$, y=0 or y=H), the boundary conditions of impermeability, rigidity, no-slip and imposed thermal gradients were used:

$$\frac{\partial \omega_i(x,0)}{\partial y} = \frac{\partial \omega_i(x,H)}{\partial y} = 0 \tag{8}$$

$$v(x,0) = v(x,H) = 0 \tag{9}$$

$$u(x,0) = u(x,H) = 0 \tag{10}$$

$$\frac{\partial T(x,0)}{\partial x} = \frac{\partial T(x,H)}{\partial x} = \frac{T_S - T_C}{L} \tag{11}$$

On the source, $(x = l\ ;\ 0 < y < H)$, the diffusion of A from the source and impermeability to B were used, in addition to no-slip and an energy balance at the crystal interface:

$$u(l,y) = -\frac{D_{AB}}{1-\omega_A(l,y)}\frac{\partial \omega_A(l,y)}{\partial x} \tag{12}$$

$$v(l,y) = 0 \tag{13}$$

$$F(l,y) - \left[k\frac{\partial T(l,y)}{\partial x}\right]_{gas} = -\left[\lambda\frac{\partial T(l,y)}{\partial x}\right]_{solid} \tag{14}$$

Analogously on the crystal, $(x = L+l\ ;\ 0 < y < H)$:

$$u(L+l,y) = -\frac{D_{AB}}{1-\omega_A(L+l,y)}\frac{\partial \omega_A(L+l,y)}{\partial x} \tag{15}$$

$$v(L+l,y) = 0 \tag{16}$$

$$F(L+l,y) - \left[k\frac{\partial T(L+l,y)}{\partial x}\right]_{gas} = -\left[\lambda\frac{\partial T(L+l,y)}{\partial x}\right]_{solid} \tag{17}$$

Boundary conditions for the source and crystal ($0 \le x \le l$; $L+l \le x \le L+2l$; $y = 0$ or $y = H$) :

$$\frac{\partial T(x,0)}{\partial x} = \frac{\partial T(x,H)}{\partial x} = \begin{cases} 0 & Case\,1 \\ \dfrac{T_S - T_C}{2l} & Case\,2 \\ \dfrac{T_S - T_C}{l} & Case\,3 \end{cases} \qquad (18)$$

with corresponding temperatures at the ampoule ends:

$$(x = 0\ ;\ 0 \le y \le H)\ ,\ T = T_s\ ;\ (x = 2L\ ;\ 0 \le y \le H)\ ,\ T = T_c \qquad (19)$$

Most of these boundary conditions have been discussed in detail in previous publications [1,4–9,11,12,14,18–20]. We will therefore comment only the new ones we are taking into account. In particular, the matching conditions at the interface between the source material and the fluid phase yields equation 14 with a source term (F(l,y)) accounting for sublimation; likewise a sink term (F(L+l,y)) also appears in equation 17 for the condensing interface at the crystal end. Note, in order to satisfy continuity the source and sink terms are compatible. Since the growth rate of the interface is much smaller than the vapor velocities, typically by three orders of magnitude, the process is quasi-steady. Thus, the term accounting for latent heat of sublimation is negligible incomparison to the conduction and advection terms. Also, similar to previous investigators we are considering that the interface remains flat during the growth of the crystal.

III. NUMERICAL FORMULATION

The system of coupled nonlinear partial differential equations has been solved using the SIMPLE algorithm (Semi-Implicit Method for Pressure-Linked Equations [22]). The conservation equations were discretized using a hybrid scheme, which provides a second-order spatial accuracy. This two-dimensional version of the algorithm uses three staggered grids, one for the scalar variables and one for each of the velocity components. In contrast to a vorticity/stream function approach, adopting a primitive variable approach allows a straightforward formulation of the velocity boundary conditions. However, the solution of the continuity equation for this problem is not automatically satisfied.

For most of the simulations, a 20x40 primary grid was used. An additional case was run with a fine 40x60 mesh. The code was run on VAX 8800 biprocessor computer, and the iterative process was stopped when a Cauchy-Schwartz type criterion was satisfied for each variable. All the results presented in this article have been obtained with a convergence criterion of 10^{-4} for each of the variables. The code was compared with a more common vorticity/stream function algorithm under the same conditions for various Grashof numbers. Results provided by the two codes differed by less than one percent [21].

IV. RESULTS AND DISCUSSION

Due to the finite value of crystal thermal conductivity, heat conduction in the crystal may affect the interface temperature and local convective patterns. We consider two cases: specifically, the flow field behavior when heat conduction is absent, and the

effect of heat conduction when longitudinal thermal gradients are applied at the crystal boundary. In the absence of heat conduction, we study the effects of the aspect ratio and the orientation of the ampoule with respect to the gravitational acceleration on thermal convection. Thermal, solutal, and thermo-solutal convection are studied in the case of a horizontal enclosure. We conclude this first part with a feasibility study of a unidirectional flow. Then, we show in the second case that when heat conduction in the crystal is present the local convection patterns are modified. However, under microgravity conditions, even in the presence of heat conduction, the flow field is restored to a unidirectional pattern.

The governing parameters of this process, i.e., the thermal and solutal Grashof numbers, can be obtained by linearizing the density field using the Boussinesq approximation:

$$\rho = \rho_0 \left(1 - \alpha(\omega^A - \omega_0^A) - \beta(T - T_0)\right) \tag{20}$$

where the subscript refers to these conditions

$$T_0 = \frac{T_C + T_S}{2} \quad \text{and} \quad \omega_0^A = \frac{\omega_A^C + \omega_A^S}{2} \tag{21}$$

The coefficients of solutal and thermal expansion are derived from the ideal gas law and may be written as follows:

$$\beta = \frac{-1}{\rho}\left[\frac{\partial \rho}{\partial T}\right]_{P,\omega_A} = \frac{2}{T_C + T_S} = \frac{1}{T_0} \tag{22}$$

$$\alpha = \frac{-1}{\rho}\left[\frac{\partial \rho}{\partial \omega_A}\right]_{P,T} = \frac{M_B - M_A}{\omega_A^0 (M_B - M_A) + M_A} \tag{23}$$

Typical operating conditions for crystal growth of mercurous chloride by Physical Vapor Transport (PVT) are shown in table 1. The vapor pressure, density and mass fraction are calculated from equations 1, 25 and 30 respectively. The total operating pressure is taken as P_{tot} = 20000 Pa; the excess pressure takes into account the effect of the residual buffer gas.

Table 1: Operating conditions and computation of mass fractions

T_c	=	537 K	T_s	=	587 K
P_A^c	=	2533 Pa	P_A^s	=	16380 Pa
ρ_c	=	0.42 kg/m^3	ρ_s	=	1.61 kg/m^3
ω_A^C	=	0.6312	ω_A^S	=	0.9812

The dimensionless parameters for the process under the conditions of this study are shown in table 2.

Table 2: Typical dimensionless parameters		
Thermal Grashof number	=	2700
Solutal Grashof number	=	10000
Prandtl number	=	0.7
Schmidt number	=	1
Aspect ratio	=	10
1 < Mass Peclet number < 30		

IV.1. Constant temperature imposed on the crystal (Case 1, $\frac{dT}{dx} = 0$)

IV.1.1. Effect of aspect ratio on interface temperature

We examine the effect of the aspect ratio on the interface temperature. The imposed thermal profile along the boundary of the enclosure is shown in Figure 2 (case 1). Parametric studies for various aspect ratios are shown in Figure 3. These cases are computed for the horizontal configuration where convection is at a maximum. The results show that in both the source material and the growing crystal, the interfacial temperature deviates more severely from a constant value as the aspect ratio decreases. The maximum temperature deviation (1.25 K) occurs for a square ampoule (Ar=1). However, for narrow ampoules with aspect ratio ≥ 10, the interfacial temperature approaches a constant value.

IV.1.2. Thermal convection in a rectangular inclined enclosure

We now investigate the flow field characteristics occurring during PVT. We simplify the calculation by assuming isothermal source and sink interfaces. This corresponds to the absence of heat conduction in the crystal. We first study extensively thermal convection.

IV.1.2.1. General pattern of thermal convection

Solutal convection is eliminated mathematically by setting the molar masses of both components to be equal: this implies $\alpha = 0$. Once we have set $M_A = M_B$, we can use a simplified formula for the density given by the ideal gas law:

$$\rho = \frac{M\ P}{R\ T} \tag{24}$$

Using this formula to compute density of vapor on both interfaces gives:

$\rho_S = 1.93\ kg/m^3$ and $\rho_C = 2.11\ kg/m^3$.

The intensity of thermal convection can be quantified using the thermal Grashof number defined as follows:

$$Gr_t = \frac{g\rho^2 H^3 \beta \Delta T}{\mu^2}$$

The pattern of convection for $Gr_t = 2672$ is shown in Figure 4.a, which exhibits the well-documented result of purely thermally driven fluid flow. The gas, lighter on the hot side, rises up along the nutrient interface, and heavier on the cold side, moves

down along the interface. Notice that the mass flux distribution, Figure 4.b, on the crystal interface exhibits significant nonuniformity. As is typical for thermal convection, more nutrient ascends to the top of the ampoule than is transported to the bottom of the ampoule. Figure 4.c shows that the convection stream modifies the mass distribution throughout the entire ampoule. Note that when $M_A = M_B$, ω ranges from .17 to .72. We conclude that thermally driven convection is the leading cause of nonuniform mass flux distribution for the case considered.

IV.1.2.2. Effect of the aspect ratio on thermal convection

From a crystal growth point of view, we would like to reduce the convection intensity in order to obtain a uniform mass flux next to the interface. One way to reduce the effect of convection is to modify the geometry of the ampoule. Aspect ratios varying from 0.5 to 20 have been studied. Figure 5 presents the velocity fields resulting from such simulations. It demonstrates that the higher the aspect ratio (length to width ratio), the lower the convection intensity. With decreasing aspect ratio, viscous effects become important and a transition to a uniform flow field results. The transition from a convective pattern (with a recirculating cell) to a diffusive pattern (uniform flow field without a recirculating cell), is observed when the aspect ratio changes from 10 to 20. The variation of mass flux with aspect ratio is shown in Figure 6. The maximum occurs for Ar=2, beyond which there is a sharp drop, and finally levels off.

IV.1.2.3. Effect of the angle between the ampoule axis and the gravity vector

The angle between the ampoule and the gravitational acceleration vector is another control parameter of the process. We have systematically studied its effect for angles varying between 0 ° (thermally stable configuration) and 180 ° (thermally unstable configuration). We operated below the critical Grashof number. As a result, these trends should be viewed as only qualitative trends, in particular, the vertical configurations.

The resulting velocity fields are represented in Figure 7. Both vertical configurations correspond to a diffusive mode of mass transport, since we are operating below the critical Grashof number. As soon as the ampoule is tilted, by as little as one degree, a recirculating cell appears. The intensity of the convection increases with slight angular variation, and peaks for an angle of 90 °. It should be emphasized that we are obtaining qualitative data from this simulation because of possible three-dimensional effects.

The distribution of the total mass flux for various angles of tilt is represented in Figure 8. The total mass flux variee between a minimum quantity, associated with the vertical configuration, and a maximum value for the horizontal configuration, which corresponds to the peak in convection levels. The minimum of the curve is sharper than the maximum, denoting the immediate transition to convection upon inclining the ampoule. Note that the total mass flux differs approximately in a proportion of 1 to 2 between the diffusive and convective modes. The mass flux distribution along the interface for various angles of tilt is shown in Figure 9. Only the vertical configuration (0 °) of the ampoule results in a uniform mass flux. This is consequently the only case in which planar growth could possibly occur.

IV.1.3. Solutal convection in a horizontal enclosure

We have already noticed from the magnitude of the thermal and solutal Grashof numbers (table 2) that solutal convection dominates thermal convection. However, to isolate the effects of solutal convection, the temperature difference between the source and the sink is set to zero, keeping the mass fraction difference equal to what was previously used. This is of course unrealistic from a physical standpoint, but our goal is to study separately each of the basic phenomena involved in crystal growth.

The formula of the density derived from the perfect gas law cannot be simplified further, and the molar mass has to be written explicitly:

$$\rho = \frac{\left[\frac{\omega_A}{m_A} + \frac{(1-\omega_A)}{m_B}\right]^{-1} P}{R\ T} \tag{25}$$

The computed densities on the interfaces are:

$$\rho_s = 1.68\ kg/m^3 \quad \text{and} \quad \rho_c = 0.41\ kg/m^3$$

The intensity of solutal convection can be quantified using the solutal Grashof number defined as follows:

$$Gr_s = \frac{g\,\rho^2 H^3 \alpha \Delta\omega_A}{\mu^2}$$

Unlike thermally driven convection, the density is greater at the hot interface than at the cold interface. We therefore expect a fluid flow and a mass flux distribution opposite to that observed for a thermally driven fluid flow. Figure 10.a presents the flow field resulting from such a theoretical hypothesis. The fluid flow moves down along the hot interface, and up along the cold interface. The maximum velocity is larger than that observed by purely thermally driven flow, indicating a stronger recirculation. This can be attributed to the larger magnitude of the Grashof number (Gr_s of order 10^5). The interfacial mass flux distribution shows that more nutrient flows to the bottom of the crystal interface than to the top of the interface (Figure 10.b), where the convective flow opposes the advection.

IV.1.4. Thermo-solutal convection in a horizontal enclosure

Physically, one cannot of course set thermal or solutal convection to zero; both are present simultaneously. With this cautionary note in mind, we proceed to choose the temperature difference between the interfaces to be 50 K, which is representative of an average growth condition. Computing densities on both interfaces gives:

$$\rho_S = 1.61\ kg/m^3 \quad \text{and} \quad \rho_C = 0.42\ kg/m^3$$

The solutal Grashof number is approximately four times greater than the thermal Grashof number (9856 vs. 2672, respectively). Thus the flow field is of solutal convection type. The mass flux distribution on the growing interface is therefore expected to be characteristic of solutally driven growth.

We have shown that, in the case we are modeling, two types of convection are competing. Our goal being to restore a uniform mass flux, we can exploit these opposing trends to eliminate their effects in the neighborhood of the growing interface. This

could theoretically be achieved if we set the Gr_t equal to the Gr_s, leading to the simple condition:

$$\beta \Delta T = \alpha \Delta \omega_A \tag{26}$$

This can be realized by increasing the temperature difference and decreasing the mass fraction difference between the two interfaces. However, this condition is not found to be sufficient to restore a uniform mass flux. A modification to equation (26) is necessary to account for the difference in mass-flux and thermal gradients; the thermal gradient of the furnace is imposed to be linear, but the mass-flux gradient has no such restriction. Most of the mass-flux gradient is localized near the interfaces, especially near the growing interface, so that the following arbitrary criterion becomes necessary:

$$\beta \Delta T = 2 \alpha \Delta \omega_A \tag{27}$$

The resulting velocity field is presented in Figure 11.a. A strong thermal recirculating cell is present throughout most of the ampoule, with a weaker recirculating region near the interface. Higher resolution studies (Figure 11.c) show that this weaker cell is unidirectional. The unidirectional flow does not occur throughout the ampoule, but is apparent close to the interface. This is enough to enable the Stefan wind to be the locally dominant mode of mass transfer. This results in a nearly planar mass flux distribution along the growing interface as shown on Figure 11.b.

IV.1.5. Feasibility of a unidirectional flow.

To achieve a flow by satisfying the pseudoequality of the thermal and solutal Grashof numbers, we had to decrease the difference in mass fraction and increase the difference in temperature between the two interfaces independently of the thermodynamical laws regulating the process. The mass fraction on the interfaces is uniquely a function of the temperatures of the interfaces through the vapor pressure law of the solid/vapor equilibrium between the solid and gas phases of component A. The pseudo-equation of equality of the thermal and solutal Grashof numbers should then be written:

$$\begin{aligned} \beta \Delta T &= 2 \alpha \Delta \omega_A \\ \beta(T_S - T_C) &= 2 \alpha (\omega_A^S - \omega_A^C) \end{aligned} \tag{28}$$

The thermodynamical vapor pressure law (equation 1) is utilized to produce the mass fraction through the following conversion equation:

$$\omega_A = \frac{P_A M_A}{P_A M_A + (P_T - P_A) M_B} \tag{29}$$

which can be rearranged to

$$\omega_A = \frac{1}{1 + \left[\frac{P_T}{P_A} - 1\right] \frac{M_B}{M_A}} \tag{30}$$

substituting equation (1), yields:

$$\omega_A = \frac{1}{1 + \left[P_T e^{\left(\frac{b}{T} - a \right)} - 1 \right] \frac{M_B}{M_A}} \tag{31}$$

If we substitute this formula in equation (28), we obtain:

$$\beta(T_S - T_C) - 2\alpha f_1(T_S, T_C) = 0 \tag{32}$$

In other words:

$$f_2(T_S, T_C, P, M_A, M_B) = 0 \tag{33}$$

We will apply this functional relationship to our particular case with the following molecular masses of $HgCl_2$ and Ar, and total pressure in the ampoule:

Table 3
P = 20000 Pa
Ma = 0.472 kg/mol
Mb = 0.04 kg/mol

We also impose the following conditions on T_S and T_C: $T_S = T_0 + \Delta T$, $T_C = T_0 - \Delta T$ with $T_0 = 562\,K$, corresponding to the working temperature of the process. The following simplified equation has to be solved:

$$f_3(\Delta T) = 0 \tag{34}$$

The solution shows that only one trivial root exists for $\Delta T = 0$. For this root, there is no driving force for the process. We conclude that, under the conditions for which we studied the process, a unidirectional fluid flow using competition between thermal and solutal convection cannot be achieved in a terrestrial environment because of a thermodynamical restriction. Other working conditions for the process have to be found.

IV.2. Imposed longitudinal thermal gradient in the crystal (Cases 2 and 3, $\left| \frac{dT}{dx} \right| > 0$)

IV.2.1. Heat conduction in the crystal, $\left| \frac{dT}{dx} \right| > 0$

The effect of heat conduction in the presence of thermal gradient on the crystal boundary (cases 2 and 3 in Figure 2) is shown in Figure 12 for the vertical configuration. These trends show that the steeper gradients increase the distortion in interface temperature. The corresponding flow field configuration for the steepest gradient (case 3) is shown in Figure 13.a. For the set of parameters chosen, the temperature gradients at the interface give rise to symmetrical cells near the interface. The core flow is the most intensive, which results in a bell shaped distribution of mass flux (Figure 13.b). In contrast to our results for the horizontal configuration which showed slight temperature deviation from a constant value at the crystal interface (case 1), the vertical configuration shows that the interface is isothermal. These slight deviations can be accounted for by the large difference in Grashof number between the two configurations. In the calculations for the vertical configuration, we selected very low temperature differences ($\Delta T = 1.5K$) to examine a limiting case for the PVT process.

IV.2.2. Microgravity environment

One of the possible alternatives is to grow the crystal in a microgravity environment. We have simulated different levels of gravity. The resulting fluid flow is shown in Figure 14 for $10^{-3}g_0$ (case 3). For gravity levels of less than $10^{-3}g_0$ (i.e., Gr < 10), no recirculating cell occurs. The corresponding mass flux distribution in front of the growing interface is therefore planar.

V. CONCLUSIONS

Considerable progress has been achieved in the past years in modeling PVT processes. Our study covers the flow field characteristics during the growth of Hg_2Cl_2 crystals in a rectangular ampoule under terrestrial and μg conditions for various imposed thermal gradients. Taking into account the real thermodynamical dependency of the mass fraction as a function of temperature reduces considerably the control we have on the process. Solutal convection becomes the main phenomenon governing the fluid flow inside the ampoule. In order to achieve our goal of a uniform mass flux near the interface (planar growth), we decided to study systematically each of the phenomenon involved in the process.

We showed that:

1. In the absence of conduction in the crystal, the interface temperature becomes uniform for Ar ≥ 10. Otherwise, in the presence of conduction when linear gradients are imposed on the crystal boundary, the interface temperature becomes non-uniform, which gives rise to multicellular convection in the flow field. The temperature distortion is proportional to the thermal gradient imposed on the crystal.

The flow field characteristics during PVT were studied by isolating the trends of thermal, solutal convection, and the combination of thermo-solutal convection. We studied thermal convection by artificially eliminating solutal convection, i.e., by setting the masses of both gas components equal. We have also shown that:

2. The magnitude of convection decreases with the aspect ratio (Ar). Up to an Ar of 10, a recirculating cell is observed. For an Ar of 20, the fluid flow switches to a diffusive mode, associated with a restored planar growth.
3. The magnitude of convection varies approximately with the sine of the angle between the ampoule and the gravitational acceleration, as does the mass flux distribution on the growing interface. The maximum mass flux occurs for the horizontal configuration. Only vertical configurations (below the critical Grashof number) provide potential for a diffusive mode of transport of mass, resulting in a uniform mass flux near the interface (planar growth).

We then studied solutal convection by restoring the mass difference and setting the temperature difference between the interfaces to zero. We have observed that for a horizontal configuration:

4. The general behavior of the fluid flow is reversed. The sense of recirculation of the flow is opposite to the one observed for thermal convection. Likewise the mass flux distribution on the growing interface follows a similar trend, where more nutrient comes on the bottom of the ampoule.

We then studied the more realistic case of a combined thermo-solutal convection in the horizontal enclosure, finding that:

5. Solutal convection was the dominant mode of the fluid flow in the ampoule.

The opposing trends of thermal and solutal convection led to the investigation of the possibility of obtaining a unidirectional flow. This was achieved by increasing the temperature difference between the two interfaces and simultaneously decreasing the mass fraction difference, independently of the requirements of the vapor pressure law. This analysis indicated that:

6. A unidirectional flow near the crystal interface is possible when the thermal Grashof number is equal to twice the solutal Grashof number under the operating conditions chosen.

We looked for the conditions of such a unidirectional flow within the framework of the thermodynamic requirements:

7. For the pressure, molar masses and temperature we are studying, such a unidirectional flow is impossible. Solutal convection always overwhelms thermal convection because of the disparity in Grashof numbers.
8. Microgravity appears to be an efficient way of resolving the problems. For gravity levels of less than $10^{-3}g_0$, the Stefan wind drives the flow. No recirculating cell can be observed, and a uniform mass flux is obtained near the interface.

Buoyancy-driven convection in PVT is almost unavoidable at 1-g because of the density gradients which are omnipresent. What are the possible actions at 1-g? Two actions come to our mind:

1. Choice of the buffer gas: most of our problems arise from the huge difference in molar mass between argon and mercurous chloride (1 to 12). We could use a heavier gas.
2. We can change the geometry of the ampoule, using the conclusion of the study of the effect of the aspect ratio (narrow ampoule).

Alternatively, the following may also be possible:

3. We can modify the partial pressures of the components. Increasing the partial pressure of component B would reduce solutal convection, but also reduce the rate of growth, the diffusion coefficient decreasing with pressure.

ACKNOWLEDGMENTS

This work was done while the first author held the position of Visiting research associate at the Universities Space Research Association. The sponsorship of both USRA and NASA Lewis Research Center are gratefully acknowledged. The authors would like to thank particularly Dr. Martin Glicksman of USRA, Dr. Mark Lee and Dr. Roger Crouch of NASA Microgravity Science and Application Division for their constant support. Mr. Thomas Glasgow, Dr. Mohammad Kassemi and Ms. Emily Nelson are thanked for their support in this work. Finally, the first author is grateful to the French Government, to the Scientific Mission in the French Embassy in Washington, to Professor Michel Gantois, to Dr. Jean-Luc Marchand and to Ms. Elizabeth Pentecost for having made this stay in USA possible.

REFERENCES

1 Klosse, K., and Ullersma, P., "Convection in a chemical vapor transport process", *Journal of Crystal Growth,* Vol. 18 (1973), pp 167-174.

2 Olson, J.M. and Rosenberger, F., "Convective instabilities in a closed vertical cylinder heated from below. Part 1. Monocomponent gases", *Journal of Fluid Mechanics,* Vol. 92 (1979), pp 609-629.

3 Olson, J.M. and Rosenberger, F., "Convective instabilities in a closed vertical cylinder heated from below. Part 2. Binary gas mixture", *Journal of Fluid Mechanics,* Vol. 92 (1979), pp 631-642.

4 Rosenberger, F., "Fluid dynamics in crystal growth from vapors", *Physico-Chemical Hydrodynamics,* Vol. 1 (1980), pp 3-26.

5 Greenwell, D.W., Markham, B.L. and Rosenberger, F., "Numerical modeling of diffusive physical vapor transport in cylindrical ampoules", *Journal of Crystal Growth,* Vol. 51 , (1981), pp 413-425.

6 Markham, B.L., Greenwell, D.W. and Rosenberger, F., "Numerical modeling of diffusive-convective physical vapor transport in cylindrical vertical ampoules", *Journal of Crystal Growth,* Vol. 51 (1981), pp 426-436.

7 Jhaveri, B.S., Markham, B.L., Rosenberger, F., "On singular boundary conditions in mass transfer across rectangular enclosures", *Chem. Eng. Commun.,* Vol. 13 (1981), pp 65-75.

8 Jhaveri, B.S., Rosenberger, F., "Expansive convection in vapor transport across horizontal rectangular enclosures", *Journal of Crystal Growth,* Vol. 57 (1982), pp 57-64.

9 Rosenberger, F. and Muller, G., "Interfacial transport in crystal growth, a parametric comparison of convective effects", *Journal of Crystal Growth,* Vol. 65 (1983), pp 91-104.

10 Muller, G., Neumann, G. and Weber, W., "Natural convection in vertical Bridgman configurations", *Journal of Crystal Growth,* Vol. 70 (1984), pp 78-93.

11 Markham, B.L. and Rosenberger, F., "Diffusive-convective vapor transport across horizontal and inclined rectangular enclosures", *Journal of Crystal Growth,* Vol. 67 (1984), pp 241-254.

12 Schaefer, R.J. and Coriell, S.R., "Convection-induced distortion of a solid-liquid interface", *Metallurgical Transaction A,* Vol 15A (1984), pp 2109-2115.

13 Huang, P.G., Launder, B.E. and Leschziner, M.A., "Discretization of nonlinear convection processes: a broad-range comparison of four schemes", *Computer Methods in Applied Mechanics and Engineering,* Vol. 48 (1985), pp 1-24.

14 Zappoli, B., "Interaction between convection and surface reactions in physical vapor transport in rectangular horizontal enclosures", *Journal of Crystal Growth,* Vol. 76 (1986), pp 449-461.

15 Bontoux, P., Roux, B., Schiroky, G.H., Markham, B.L. and Rosenberger, F., "Convection in the vertical midplane of a horizontal cylinder. Comparison of two-dimensional approximations with three-dimensional results", *International Journal of Heat Mass Transfer,* Vol. 29 (1986), pp 227-240.

16 Henry, D. and Roux, B., "Three-dimensional numerical study of convection in a cylindrical thermal diffusion cell: its influence on the separation of constituents", *Physics of Fluids,* Vol. 11 (1986), pp 3562-3572.

17 Singh, N. B., Hopkins, R.H., Mazelsky, R., and Glicksman, M.E., "Convection and diffusion effects during Physical Vapor Transport of Hg_2Cl_2 ", *Mat. Res. Soc. Symp. Proc.*, Vol. 87 (1987), pp 71-76.

18 Extremet, G.P., Roux, B., Bontoux, P. and Elie, F., "Two-dimensionnal model for thermal and solutal convection in a multizone Physical Vapor Transport", *Journal of Crystal Growth*, Vol. 82 (1987), pp 761-775.

19 Kassemi, M and Duval, W.M.B., "Effect of gas and surface radiation on crystal growth from the vapor phase", presented in the *7th Physico-Chemical Hydrodynamics Meeting*, MIT, Cambridge, Massachusetts, July 25-29, 1989.

20 Kassemi, M. and Duval, W.M.B., "Interaction of surface radiation with convection in crystal growth by physical vapor transport", AIAA Paper 89-0228, presented in the 27th AIAA Aerospace Sciences Meeting, Reno, Nevada, January 1989. Also *AIAA Journal of Thermophysics and Heat Transfer*, (in press: April 1990)

21 Mennetrier, C., "*Etude cinetique et modelisation du procede van Arkel. Application a la purification du hafnium*", Ph.D. Dissertation, Institut National Polytechnique de Lorraine (France), 1988.

22 Patankar, S.V., "*Numerical Heat Transfer and Fluid Flow*", Mac Graw-Hill, 1980.

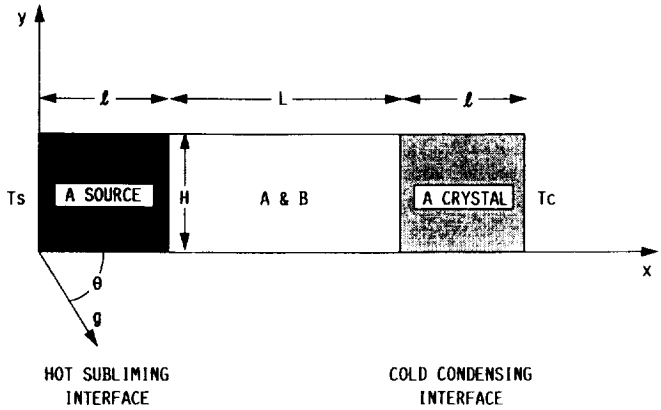

Figure 1.—Physical vapor transport enclosure.

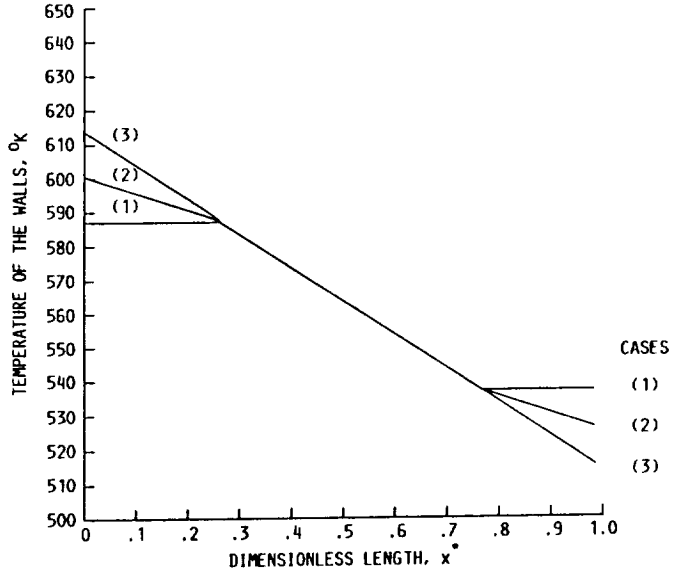

Figure 2.—Temperature profile along the ampoule.

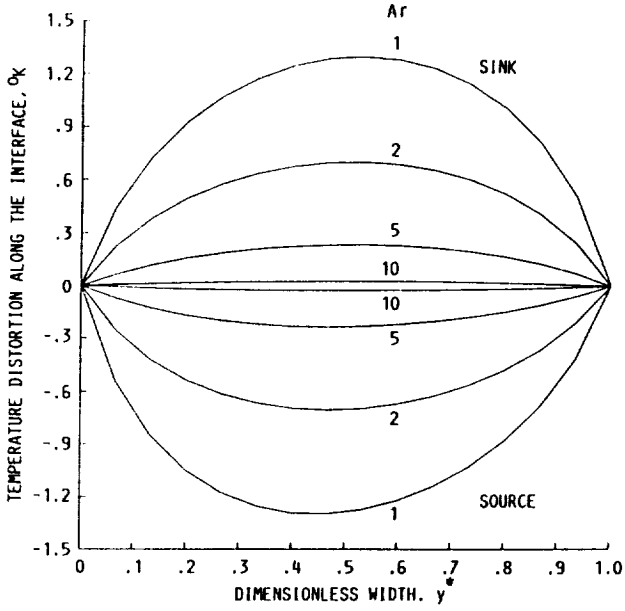

Figure 3.—Resulting temperature profiles of the crystal interface for various aspect ratios.

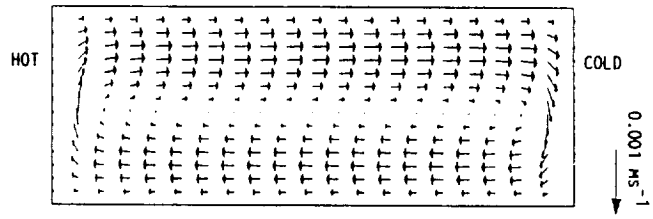

(a) Thermal convection driven fluid flow (Gr_t = 2672, Gr_s = 0, Gr_s/Gr_t = 0, Ar = 10).

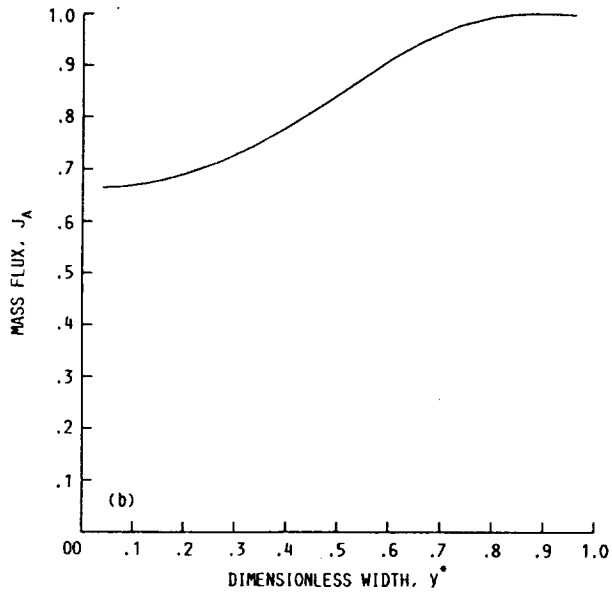

(b) Mass flux distribution along the growing interface (J_{max} = 1.37x10^{-1} mol/s-m^2).

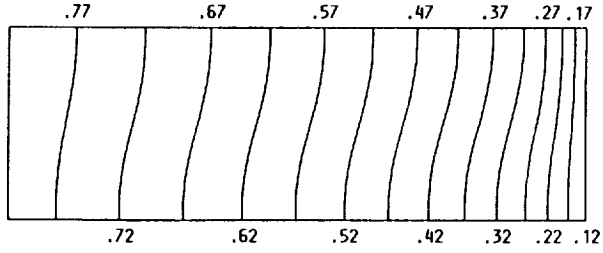

(c) Mass fraction contours in the ampoule.

Figure 4.

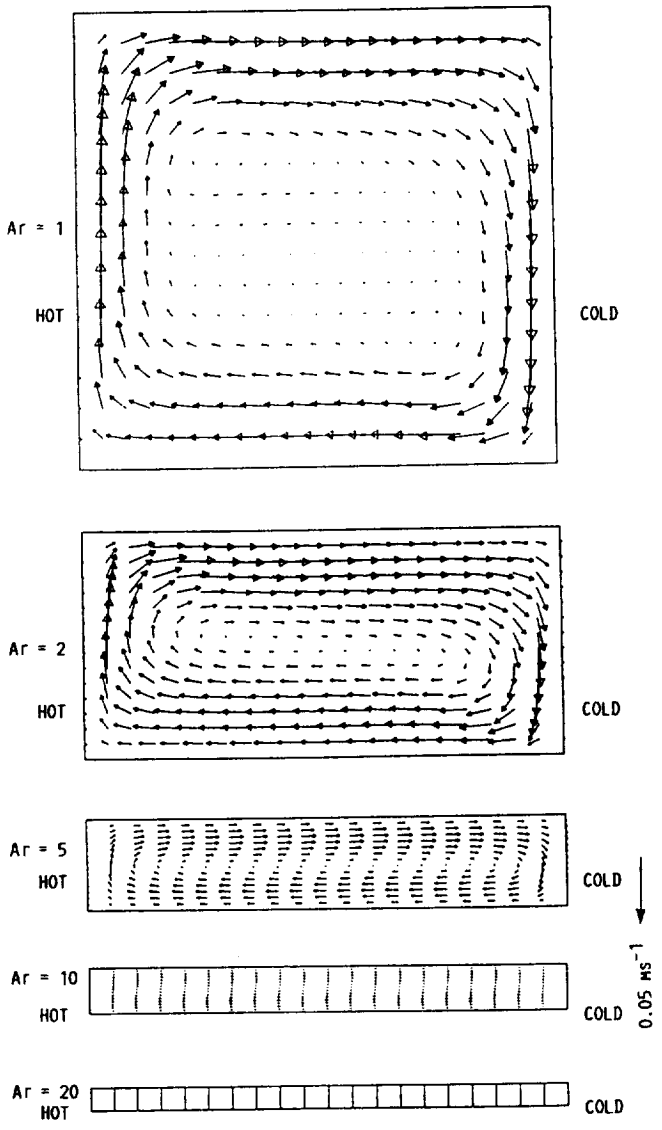

Figure 5.—Effect of the aspect ratio on the fluid flow (For Ar = 1, 2, 5, 10, and 20 the corresponding Grashof numbers are Gr_l = 2.672 10^6, 3.34 10^5, 2.138 10^4, 2.672 10^3, 3.34 10^2 respectively).

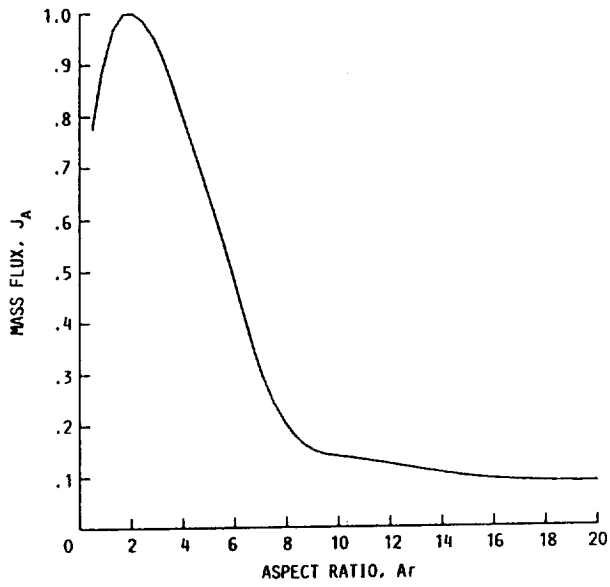

Figure 6.—Mass flux versus aspect ratio (J_{max} = .25x10^{-1} mol/s-m^2).

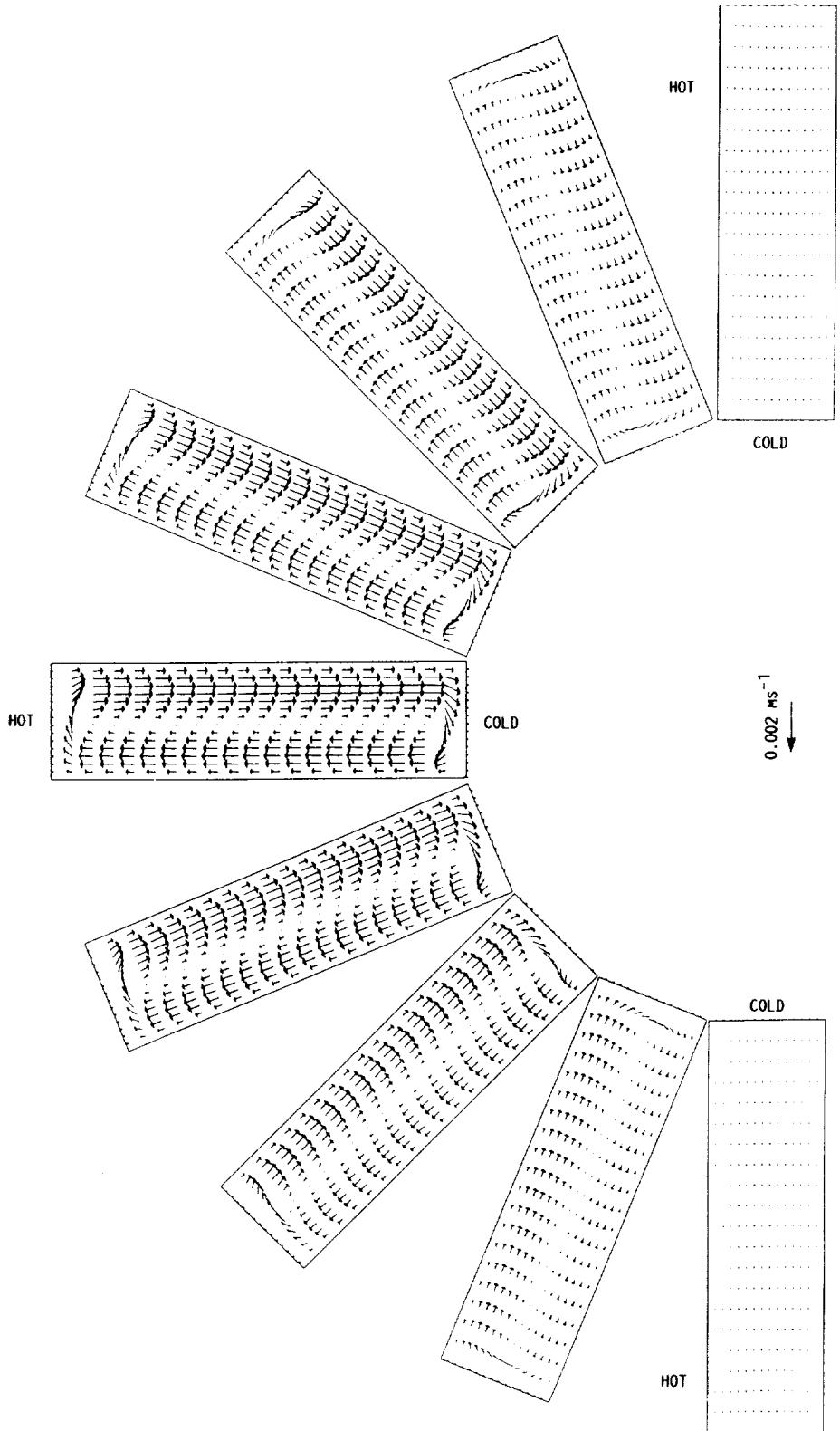

Figure 7.—Effect of the angle of tilt on the fluid flow (Ar = 10). Thermally stable (0°) to unstable (180°) mode vary counterclockwise from the top to the bottom respectively,

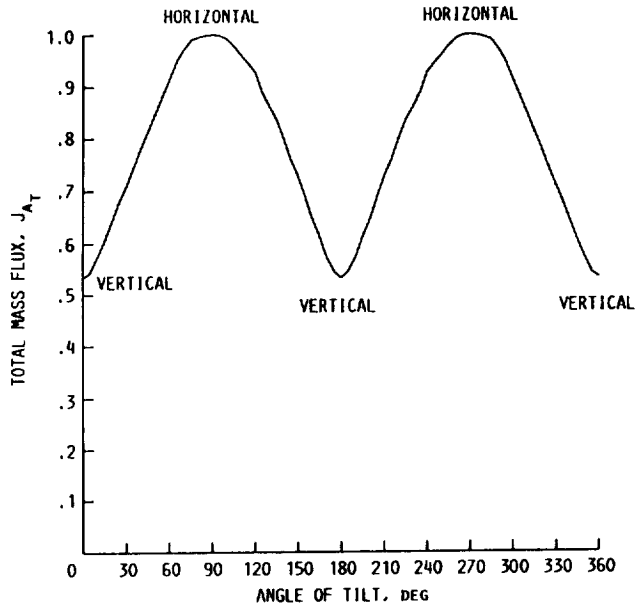

Figure 8.—Effect of the angle of tilt on the total mass flux inside the enclosure (Ar = 10).

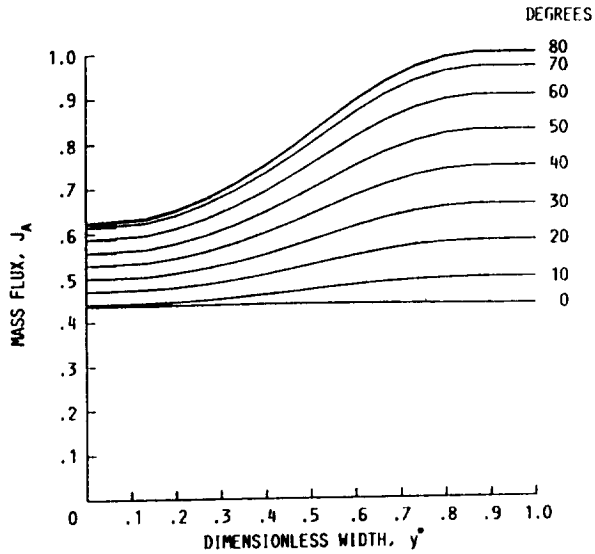

Figure 9.—Effect of the angle of tilt on the nonuniformity of the mass flux on the growing interface (Ar = 10, J_{max} = .38x10^{-1} mol/s-m^2).

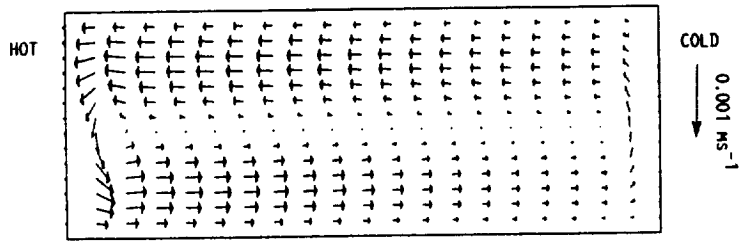

(a) Fluid flow driven buy solutal convection (Gr_t = 0, Gr_s = 9856, Gr_s/Gr_t = ∞, Ar = 10).

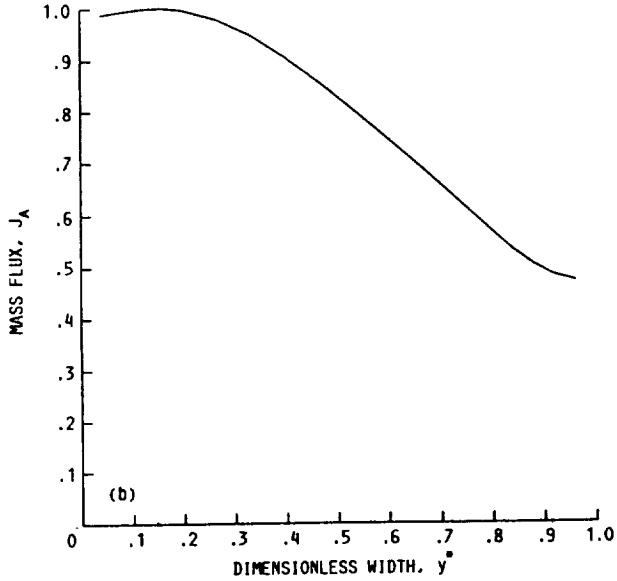

(b) Corresponding mass flux distribution along the growing interface (J_{max} = 1.5x10^{-1} mol/s-m^2).

Figure 10.

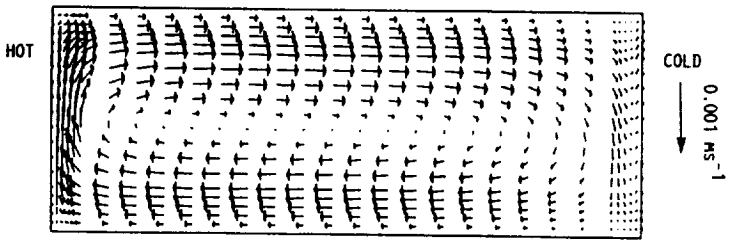

(a) Thermo-solutal flow field (Gr_t = 2672, Gr_s = 1336, Gr_s/Gr_t = 0.5, Ar = 10).

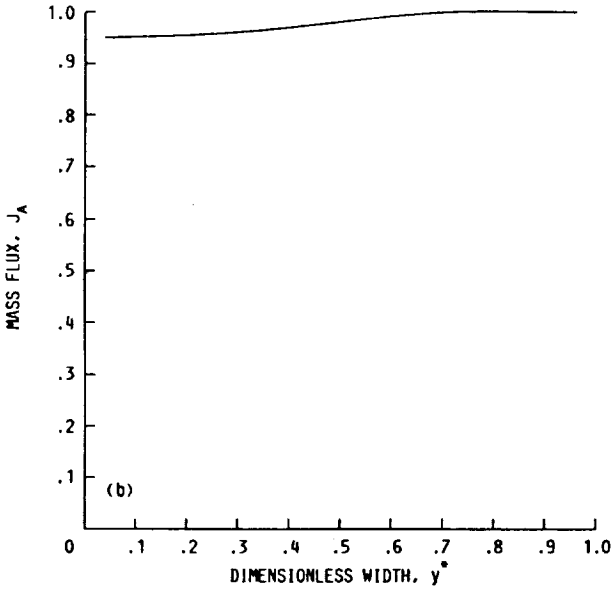

(b) Corresponding mass flux distribution along the growing interface (J_{max} = 1.35x10^{-1} mol/s-m^2).

Figure 11.

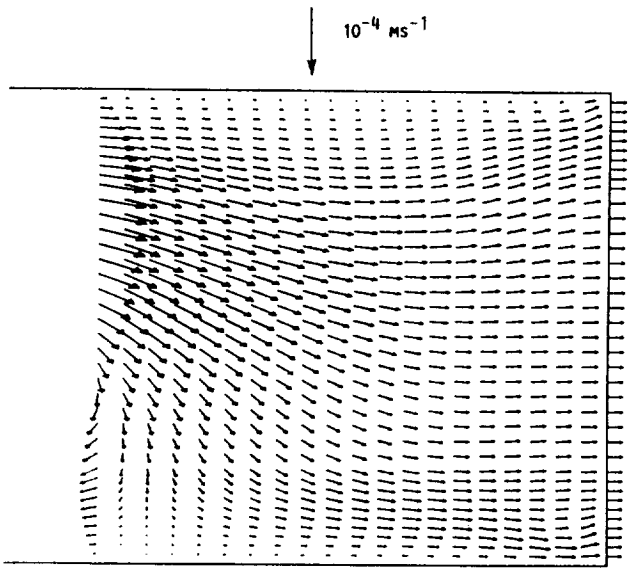

FIGURE 11c.

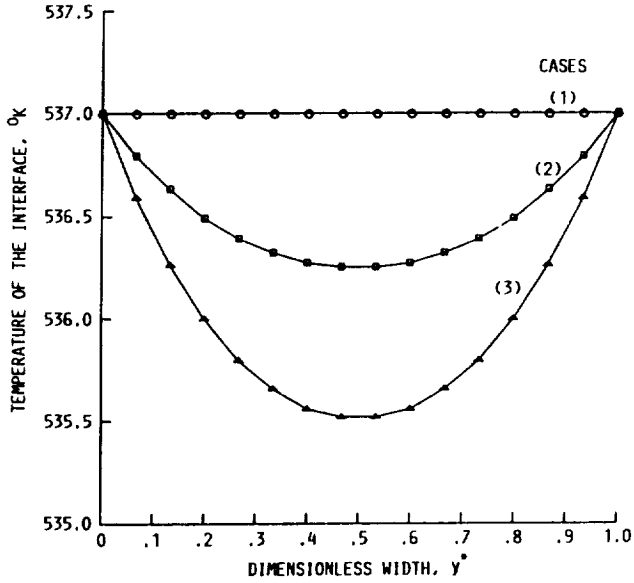

Figure 12.—Resulting temperature profiles of the crystal interface for various temperature gradients, cases (1), (2), and (3) correspond to $\frac{dT}{dx}$ = 0, -2.5, and -5 °Kcm^{-1} respectively.

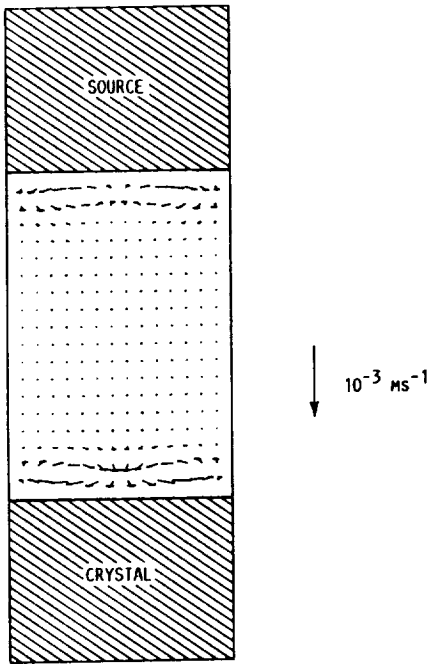

(a) Effect of thermal gradient in the crystal on the flow field (Gr_t = 350, Gr_s = 0, Gr_s/Gr_t = 0, Ar = 10).

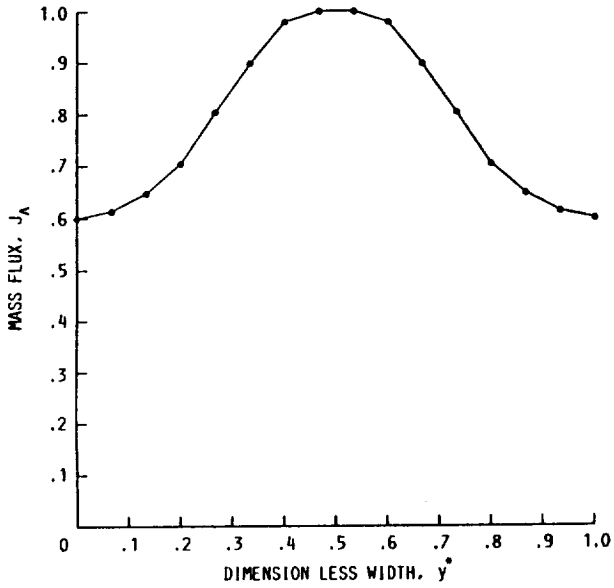

(b) Corresponding mass flux distribution along the growing interface.

Figure 13.

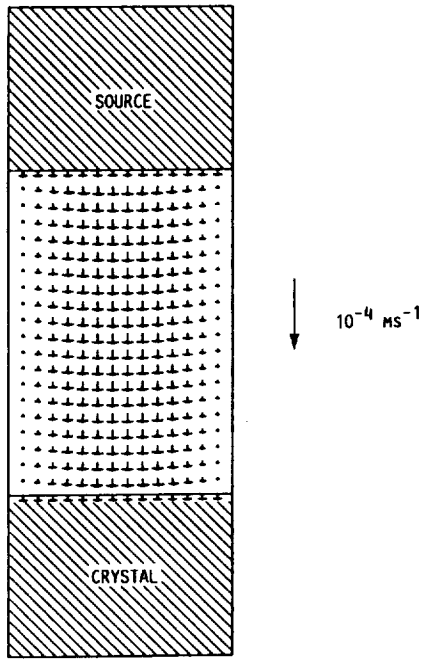

Figure 14.—Microgravity environment fluid flow (10^{-3} g_o, Gr_t = 10).

REPORT DOCUMENTATION PAGE

Form Approved
OMB No. 0704-0188

1. AGENCY USE ONLY (Leave blank)	2. REPORT DATE	3. REPORT TYPE AND DATES COVERED
	December 1991	Technical Memorandum

4. TITLE AND SUBTITLE

Thermal and Solutal Convection With Conduction Effects Inside a Rectangular Enclosure

5. FUNDING NUMBERS

WU-674-21-05

6. AUTHOR(S)

Christophe Mennetrier and Walter M.B. Duval

7. PERFORMING ORGANIZATION NAME(S) AND ADDRESS(ES)

National Aeronautics and Space Administration
Lewis Research Center
Cleveland, Ohio 44135-3191

8. PERFORMING ORGANIZATION REPORT NUMBER

E-5521

9. SPONSORING/MONITORING AGENCY NAMES(S) AND ADDRESS(ES)

National Aeronautics and Space Administration
Washington, D.C. 20546-0001

10. SPONSORING/MONITORING AGENCY REPORT NUMBER

NASA TM-105371

11. SUPPLEMENTARY NOTES

Christophe Mennetrier, Visiting Research Associate, Ecole Nationale Superieure des Mines, France at NASA Lewis Research Center. Walter M.B. Duval, NASA Lewis Research Center. Responsible person, Walter M.B. Duval, (216) 433-5023.

12a. DISTRIBUTION/AVAILABILITY STATEMENT

Unclassified - Unlimited
Subject Category 34

12b. DISTRIBUTION CODE

13. ABSTRACT *(Maximum 200 words)*

We investigate numerically the effects of various boundary conditions on the flow field characteristics of the Physical Vapor Transport process. We use a prescribed temperature profile as boundary condition on the enclosure walls, and we consider parametric variations applicable to ground-based and space microgravity conditions. For ground-based applications, density gradients in the fluid phase generate buoyancy-driven convection which in turn disrupts the uniformity of the mass flux at the interface depending on the orientation. Heat conduction in the crystal can affect the fluid flow near the interface of the crystal. When considering isothermal source and sink at the interfaces, we observe a diffusive mode and three convective modes (i.e., thermal, solutal and thermo-solutal). The convective modes show opposing flow field trends between thermal and solutal convection; theoretically, these trends can be used to achieve a uniform mass flux near the crystal. However, under the physical conditions chosen, the mathematical condition necessary for uniform mass flux cannot be satisfied because of thermodynamic restrictions. When a longitudinal thermal gradient is prescribed on the boundary of the crystal a non-uniform interface temperature results, which induces a symmetrical fluid flow near the interface for the vertical case. For space microgravity applications, we show that the flow field is dominated by the Stefan wind and a uniform mass flux results at the interface.

14. SUBJECT TERMS

Physical vapor transport; Crystal growth; Thermo-solutal convection

15. NUMBER OF PAGES

24

16. PRICE CODE

A03

17. SECURITY CLASSIFICATION OF REPORT	18. SECURITY CLASSIFICATION OF THIS PAGE	19. SECURITY CLASSIFICATION OF ABSTRACT	20. LIMITATION OF ABSTRACT
Unclassified	Unclassified	Unclassified	